Global crop production: adaptation to temperature increase is possible by maintaining the current growing periods

Running title: Crop adaptation to temperature increase

Sara Minoli[1,*] Christoph Müller[1] Joshua Elliott[2]
Alex C. Ruane[3] Jonas Jägermeyr[3] Florian Zabel[4]
Marie Dury[5] Christian Folberth[6] Louis Francois[5]
Tobias Hank[4] Ingrid Jacquemin[5] Wenfeng Liu[7]
Stefan Olin[8] Thomas A. M. Pugh[9]

[1] Potsdam Institute for Climate Impact Research (PIK), P.O. Box 60 12 03, D-14412, Potsdam, Germany
[2] University of Chicago & Argonne Natl. Lab Computation Institute, Chicago, Illinois, USA
[3] National Aeronautics and Space Administration Goddard Institute for Space Studies, New York, NY, United States
[4] Department of Geography Ludwig-Maximilians-Universität München (LMU Munich), Münich, Germany
[5] Unité de Modélisation du climat et des Cycles Biogéochimiques, UR SPHERES, Université de Liège, Quartier Agora, Allée du Six Août 19 C, B-4000 Liège, Belgium
[6] International Institute for Applied Systems Analysis, Ecosystem Services and Management Program, Schlossplatz 1, A-2361 Laxenburg, Austria
[7] Eawag, Swiss Federal Institute of Aquatic Science and Technology, Ueberlandstrasse 133, CH-8600 Duebendorf, Switzerland
[8]
[9]

∗ corresponding author: sara.minoli@pik-potsdam.de

Abstract

Increasing temperature trends are expected to impact yields of major field crops by affecting various plant processes, such as phenology and growth. However future projections, especially at the global scale, do not consider any agronomic adaptation in farming practices. We use an ensemble of seven Global Gridded Crop Models (GGCMs) contributing to the AgMIP-Gridded project to quantify the impacts and adaptation potential of field crops under increasing temperature. We study how uniform warming scenarios up to 6 K affect the productivity and growing period duration of five major crops. The design of the experiment aims at understanding adaptation measures targeted to temperature-driven impacts and therefore leaves out changes in any other climate variable. We find that, without adaptation the dominant effect of temperature increase is to shorten the growing period and to reduce yields and production, consistently across crops and regions. We then test the potential of two agronomic measures to contrast warming-induced yield reduction, assuming that (i) cultivars with adjusted phenology would be used to regain the reference growing period duration; (ii) rainfed systems would be converted to irrigated. Despite substantial uncertainties in model parametrization and little agreement in spatial patterns, at the global aggregation, model results are robust. We find that up to 3 K of temperature increase, production losses could be fully compensated by maintaining the original crop growing period. Irrigation would also compensate production losses, but would not reduce the temperature impacts. Across regions, the model ensemble estimates larger adaptation potentials from unchanged growing periods in continental and temperate regions, than in tropical and arid regions, where also irrigation has respectively little effects and availability.

Keywords: temperature increase, crop yield, adaptation, growing period, irrigation

1 Introduction

Productivity of current cropping systems can be severely affected by changes in climatic and weather variables (Challinor et al., 2014; Rosenzweig et al., 2014). Increasing temperature trends have already negatively impacted productivity of agricultural crops over the last decades (Lobell et al., 2011). Multiple methodologies consistently estimate that each degree-Celsius warming causes an average 6% decline in yields of major cereal crops, if no adaptation measures are undertaken (Liu et al., 2016; Zhao et al., 2017). Future projections indicate that large portions of current global harvested area will continue experiencing declines in the attainable yields. This even if assuming that e.g. current management was transferred among regions to adapt to climate change (Pugh et al., 2016).

The crop yield is a result of several physiological plant processes, many of which are mediated by the ambient temperature, as plants can only partially internally regulate their own temperature (Parent et al., 2010). Temperature increases up to process-specific optimum are associated with accelerated rates of (i) crop phenological development (the progress through the life cycle stages of the plant), (ii) growth metabolism (e.g. photosynthesis and respiration) and (iii) evapotranspiration (Asseng et al., 2015; Eyshi Rezaei et al., 2015; Wang et al., 2017). If on the one hand higher metabolic and transpiration rates can enhance primary productivity (biomass) per unit of time, on the other hand faster phenology determines shorter crop growing period durations (time from sowing to maturity), which are often associated to lower productivity (Hatfield et al., 2011; Egli, 2011). Moreover increased evapotranspiration rates can faster deplete the soil water content, possibly leading to plant water stress. In consequence, different agronomic management options are proposed as adaptation strategies against temperature induced yield decrease. Most commonly these include shift of sowing dates, choice of cultivar with adjusted phenology and irrigation.

Although some literature has been produced on the assessment of the above mentioned adaptation strategies at scales from local to regional (Semenov et al., 2014; Burke & Emerick, 2016; Ruiz-Ramos et al., 2018; Parent et al., 2018), their study at the global scale remains an open question. As a consequence, global projections of climate change impacts normally do not consider the adaptation of agricultural system in response to climate change and might therefore overestimate impacts on crop yields and production.

Crop models allow to conduct virtual experiments controlling by several factors, to study the complex biophysical effects of atmosphere and soil processes on crop growth and productivity. As such, they are widely applied methods for the analysis of climate change impacts on agriculture and play a fundamental role in integrated assessment studies (Rosenzweig et al., 2018). Here we propose the first spatially-explicit global study of the adaptation potential to local temperature increase of current rainfed systems. We use results from Global Gridded Crop Models (GGCMs) participating to the Agricultural Model Intercomparison and Improvement Project (AgMIP) (Rosenzweig et al., 2013). The aims of the study are to assess the potential of adaptation in growing period selection and supplementary irrigation to avoid warming-induced reductions in crop yields. To this end, we study how uniform warming scenarios of 1, 2, 3, 4, and 6 K affect crop productivity and growing period duration. We then compare this to a set of scenarios where different (hypothetical) cultivars with adjusted phenology are introduced, which maintains the reference growing period. As a second adaptation measure we study the effect of irrigation. Both adaptation measures are analyzed separately and jointly. Since crop model responses are uncertain and model often show complementary skills (Müller et al., 2017),

we make use of a large ensemble of GGCMs. These have run protocol-based simulations, harmonizing for input data on both weather variables and agronomic management settings. Using a crop ensemble, we can address the model-induced uncertainty of our findings.

1.1 Materials and methods

1.1.1 Simulation protocol and Models

Seven GGCM frameworks (CARAIB, GEPIC, LPJ-GUESS, LPJmL, pDSSAT, PEPIC, PROMET) are contributing to this study (Tab. 1) and follow the GGCMI phase 2 simulation protocol (SI, section 5.1). All simulations are run at 0.5 degree spatial resolution and for 31 years of the historical climate (1980-2010), models with a daily time step use AgMERRA (Ruane et al., 2015), while those with three hourly time resolution use ERA-Interim (ERAI) (Weedon et al., 2014). The experiment design consists of separate simulations for five crops (maize, rice, soy, spring-wheat, winter-wheat), under six levels of globally uniform temperature increases (T0, T1, T2, T3, T4, T6) and four management settings, that we call *historical-management* setting (*T-sensitive growing period* & *Rainfed*) and three *adaptive-management* setting (*Fixed growing period* & *Rainfed*; *T-sensitive growing period* & *Irrigation*; *Fixed growing period* & *Irrigation*). To target specific adaptation strategies it is necessary to isolate the the effect of individual climatic factors, as there is uncertainty in e.g. the temperature sensitivity to increased CO_2 and in future correlations between precipitation and temperature patterns (Carter et al., 2016; Zhao et al., 2017; Schleussner et al., 2018). In this study we aim at isolating the impact and adaptation of crops to temperature increase. Therefore, the atmospheric CO_2 concentration is kept constant at 360 ppm in all simulation years and scenarios. Similarly, precipitation and other climate drivers are unchanged across scenarios.

The model ensemble is harmonized for some key management practices: 1) the growing period; 2) the water supply (rainfed or fully irrigated); 3) the nitrogen-fertilizer application rate. The growing period harmonization follows the protocol of phase 1 (Elliott et al., 2015), based on observed growing period data (Sacks et al., 2010; Portmann et al., 2010), gap-filled with rule-based (Waha et al., 2012) cropping calendars. Modellers are asked to calibrate the phenology, so that the average (over the 31-years simulation period) growing periods match the provided crop- and grid-specific sowing and maturity dates. Maturity dates are estimated from observed harvest dates by subtracting crop-specific maturity to harvest times (21, 7, 21, 7, 7 days for maize, rice, soy, spring-wheat, winter-wheat respectively) (Elliott et al., 2015). The calibration procedure is individually chosen by each modelling team, which can freely determine phenological parameters such as cardinal temperatures, growing degree days, vernalization and/or photoperiod requirements, as well as set these as grid-specific or as global values. The obtained parametrization is assumed to describe the available historical crop cultivar pool, see detail in Table 1 and S3. Irrigation is assumed to be unconstrained by surface water availability and each crop is simulated under rainfed and fully irrigated conditions in each grid cell. Current cropland patterns are selected in model post-processing. The nitrogen load is assumed to be 200 kgN ha^{-1} y^{-1} uniformly for each crop and cropping season, applied in 2 doses: 50% at planting, 50% on a crop- and grid-specific day (see protocol in SI, section 5.1).

Five artificial warming scenarios are created by perturbing input daily air temperature by five respective offsets (+1, +2, +3, +4, +6 K).

In addition to simulations assuming *historical management*, three *adaptive management* scenarios are simulated for each temperature level: 1) under the *fixed growing period* setting we assume the use of different hypothetical cultivars with adapted phenological traits, which maintain the reference growing period under each warming level; 2) under the *irrigation* setting we assume the supply of unlimited irrigation water to the crops; 3) we also test the combination of *fixed growing period* and *irrigation*. The textitfixed growing period implementation is simulated by adjusting the crop phenological parameters, so that the average (over the 31-years simulation period) length of the growing period (in days) is the same (as closely as possible) under all T0-T6 scenarios. Modellers are asked to implement individual solutions to maintain the current growing period extent (e.g. precalculating changes in thermal time requirements based on fixed temperature shifts or adjusting by iteration). For models that separate phenology into multiple stages (e.g. sowing-to-anthesis and anthesis-to-maturity) modelers are asked to scale parameters of each stage equally, so that the timing of intermediate stages such as anthesis stays approximately the same. Sowing dates are kept constant at the historical observations. *Irrigation* is implemented to re-fill soil water content to field capacity as soon as it falls below a threshold of 90% of soil field capacity (Elliott et al., 2015).

Table 1: GGCMs participating in the study with main features of their phenological module.

GGCM	Temperature response function	Phenological drivers	Perceived Temperature	Phenological phases
CARAIB	Lin., Tmin	T(GDD), W	Tair	1 (S-M)
GEPIC	Lin., Tmin, Topt	T(GDD), T(V), DL	Tair	1 (S-M)
LPJ-GUESS	Lin., Tmin, Topt*, Tmax*	T(GDD), T(V)	Tair	2 (S-A-M)
LPJmL	Lin., Tmin	T(GDD), T(V)	Tair	1 (S-M)
pDSSAT	[?]	[T(GDD), T(V), DL, O]	Tair	[?]
PEPIC	Curv., Tmin, Topt	T(GDD), W, N	Tair	1 (S-M)
PROMET	Curv., Tmin, Topt, Tmax	[T(DVR)], T(V), DL, W	Tleaf	10 (BBCH)

Temperature response function for phenology (Wang et al., 2017): Lin, linear; Curv., curvilinear; Tmin; minimum cardinal temperature; Topt, optimum cardinal temperature; Tmax, maximum cardinal temperature; * for spring-wheat and winter-wheat only

Phenological drivers: T(GDD), temperature (growing degree days); T(DVR), temperature (development rate); T(V), temperature (vernalization); DL, daylength; W, water; N, nitrogen

Perceived temperature: Temperature perceived by the crop, driving phenological and metabolic processes (Tair, air temperature; Tleaf, leaf temperature)

Phenological phases: S, sowing; A, anthesis; M, maturity; BBCH, full BBCH

1.1.2 Model output processing

Models report yearly dry-matter yields ($MgDM\ ha^{-1}$), sowing dates (day of year, DOY), maturity-dates ($days\ from\ planting$) for the period 1980-2010, separately for maize, rice, soy, spring-wheat, winter-wheat. Yield failures are reported as 0 $Mg\ ha^{-1}$, while non-simulated grids are reported as NA values. Maturity dates of yield failure years are set to NA.

We compute the long-term averages (1980-2009) for yield, sowing date and maturity date for the period 1981-2009 for each model, temperature offset scenario, and manage-

ment setting respectively. The first and last year of the simulation time series are excluded to ensure a complete growing season associated reporting issue (Elliott et al., 2015).

Under the reference temperature scenario ($T0$) the growing periods are assumed to be the same as in all management settings. Yields of *fixed growing period* are assumed to be the same as in *T-sensitive growing perios* for the *rainfed* and *irrigation* settings respectively. Outputs for $T5$ are not simulated, and therefore derived by linear interpolation between $T4$ and $T6$ for each GGCM, crop and grid cell, independently for each of the management setting (categorical variables). Some are not available for all models (Fig. S1), and we gap-filled missing simulations by linear interpolation of neighboring scenarios (with an exception for rice and soy for the LPJ-GUESS model that are not simulated at all). The CARAIB model has a partially harmonized growing period (with harmonized sowing dates, while the model was not calibrated to match observed harvest dates, see Section 5.2.1 for details), but the simulation with *fixed growing periods* as needed.

For data processing we use R (R Core Team, 2018), and R-packages for handling netcdf4 (Pierce, 2015), for handling big-data and perform computation (Dowle & Srinivasan, 2017; Wickham, 2011) and for plotting results (Wickham, 2009).

1.1.3 Metrics

All GGCMs included in this study simulate crop phenology as a function of temperature (thermal-unit sum, vernalization). We quantify the average impact of globally uniform temperature increase on growing periods and yields across all GGCMs and cropland-grid cells by fitting linear regression models for each individual crop (Fig. 2a,b). To understand whether there is a direct relationship between responses of growing periods and yields to temperature increase, we analyze the joint distribution of their changes from the reference scenario (T0). We categorize the possible responses into four classes, defined by the sign of change of the two variables, and illustrate their frequency of occurrence within each class and climatic regions (Fig. 2c).

To quantify the impact of temperature increase on global crop production, we estimate the production change (%) under warming scenarios as compared to the reference temperature scenario (T0). The grid-based global production under the management system m and temperature offset n ($P_{m,n}$, Eq. (1)) is obtained as the sum of production across all crops (c) and grid cells (g). Within the grid cell j, the yield of crop i is multiplied by its calorie content and by its area in that grid.

$$P_{m,n} = \sum_{j=1}^{g} \sum_{i=1}^{c} area_{j,i} \cdot yield_{j,i} \cdot calorie_i \tag{1}$$

The calorie content values are derived from the FAO food balance sheet handbook (FAO, 2001), which reports food composition in terms of weight "as purchased", therefore model output yields are converted from dry- to fresh-matter as from Wirsenius (2000) to obtain the calorie-yield per crop and unit of area (Tab. 2). The grid cell- and crop-specific area is obtained from MIRCA2000 (Portmann et al., 2010) data set at 0.5 degree resolution.

To determine whether the *fixed growing period* and *irrigation* can be effective adaptation options we compute the *Adaptation Index* (AI, Eq. (2)) (modified from Lobell (2014)) for each grid cell, temperature offset, and *adaptive management* setting as

$$AI = 100 \cdot (c - b)/|a|, \text{ if } a < 0 \tag{2}$$

Table 2: Crop parameters used for post-processing model outputs.

Crop	Grain dry matter (%)	Calorie content (Gcal Mg^{-1})
maize	88	3.560
soy	91	3.350
spring-wheat	88	3.340
winter-wheat	88	3.340
rice	87	2.800

where a is the impact of temperature increase on yield under *historical management*, b is the effect of the *adaptive management* under the reference scenario T0, c is the effect of the *adaptive management* under increased temperature scenarios (Fig. 1). Values of AI are computed only if a is negative, otherwise temperature increase is considered beneficial and no adaptation measures are necessary. AI ranges between $-\infty$ and $+\infty$, with $AI \geq 100$ indicating full- or over-compensation of losses (full adaptation); $0 < AI < 100$ indicating partial-compensation of losses (partial adaptation); $AI < 0$ indicating no-compensation of losses, meaning either an amplification of damages or that the adaptive-management can be increasing production, without being impact-reducing (intensification), and therefore not a true adaptation measure. AI is computed for each single GGCM and we then compute the median ensemble and uncertainty (two model-standard deviations) across GGCMs.

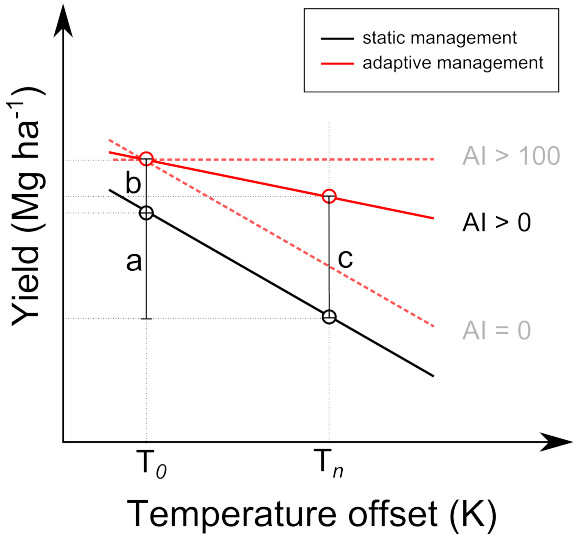

Figure 1: Diagram of the Adaptation Index (AI) computation (Modified from Lobell (2014)). The plot shows the yield (Mg ha^{-1}) as a function of increasing temperature offsets (K). T_0 is the temperature under the reference climate, T_n is the temperature under a warmer climate (in this study T_n represents increasing temperature offsets of T1 to T6). The black and the red line represent the Yield~Temperature curves with either *historical* or *adaptive* crop management. AI is computed as in Eq. 2 where a is the impact of temperature increase from T0 to Tn on yield under static management, b is the effect that the adaptive management would have under the reference conditions (T0), c is the effect that the adaptive management would have under warmer climate Tn.

2 Results

2.1 Crop phenology response to temperature offsets

With increasing temperature, the growing period shortens almost linearly at the global aggregation (Fig. 2). The slope of this relationship (days of growing period lost per degree of warming) is very similar across the five crops considered here, ranging between 5.4 $days\,K^{-1}$ (maize) and 3.8 $days\,K^{-1}$ (spring-wheat). The spread of growing period length across all GGCMs and all cropland globally does not change much with warming (whiskers in Fig. 2), except for soy, where the spread increases and winter-wheat, where it slightly decreases with temperature. There are differences between models S4. The general response is robust across the GGCMs (Tab. 1) with a linear temperature response function, whereas PEPIC and PROMET, which both implemented a curvilinear function of phenology show smaller (or even opposite in case of rice, PROMET) sensitivity of the growing period change across crops. Spatial patterns of growing period length at different temperature levels show that its shortening (days) is especially pronounced in cold-temperature limited regions for maize and soy (Fig. S8a), because less days are below base temperatures under warming there.

2.2 Impact of temperature offsets on crop yield

The response in crop yields follows a very similar pattern as the growing period, with an almost linear decline with temperature. Here differences between crops in temperature-induced yield losses range between 0.36 t ha^{-1} K^{-1} for rice and 0.11 t ha^{-1} K^{-1} for winter-wheat (Fig. 2b). Also the spread of crop yield across all GGCMs and all cropland globally decreases with temperature, by simply approaching lower yield levels and thus display reduced spread at the low end of the distribution. For rice, soy and winter-wheat, we also observe narrower interquartile ranges (boxes in Fig. 2b) with temperature.

There is no clear relationship between changes in growing period and changes in crop yields, however in most cases (69%) shorter growing periods are associated with declining yields (Fig. 2c): 71, 62, 68, 70, and 12 % for tropical, arid, temperate, continental and polar areas respectively. There are rare cases where decreasing growing periods are associated with increasing yields or where longer growing periods are associated with declining yields. However, longer growing periods with increasing crop yields are basically non-existent. In some GGCMs, phenology is implemented to slow down at high temperatures (Tab. 1), so that warming can also lead to longer growing periods. Also, for winter-wheat, vernalization requirements are not satisfied as quickly under warming, so that the phenological development decelerates.

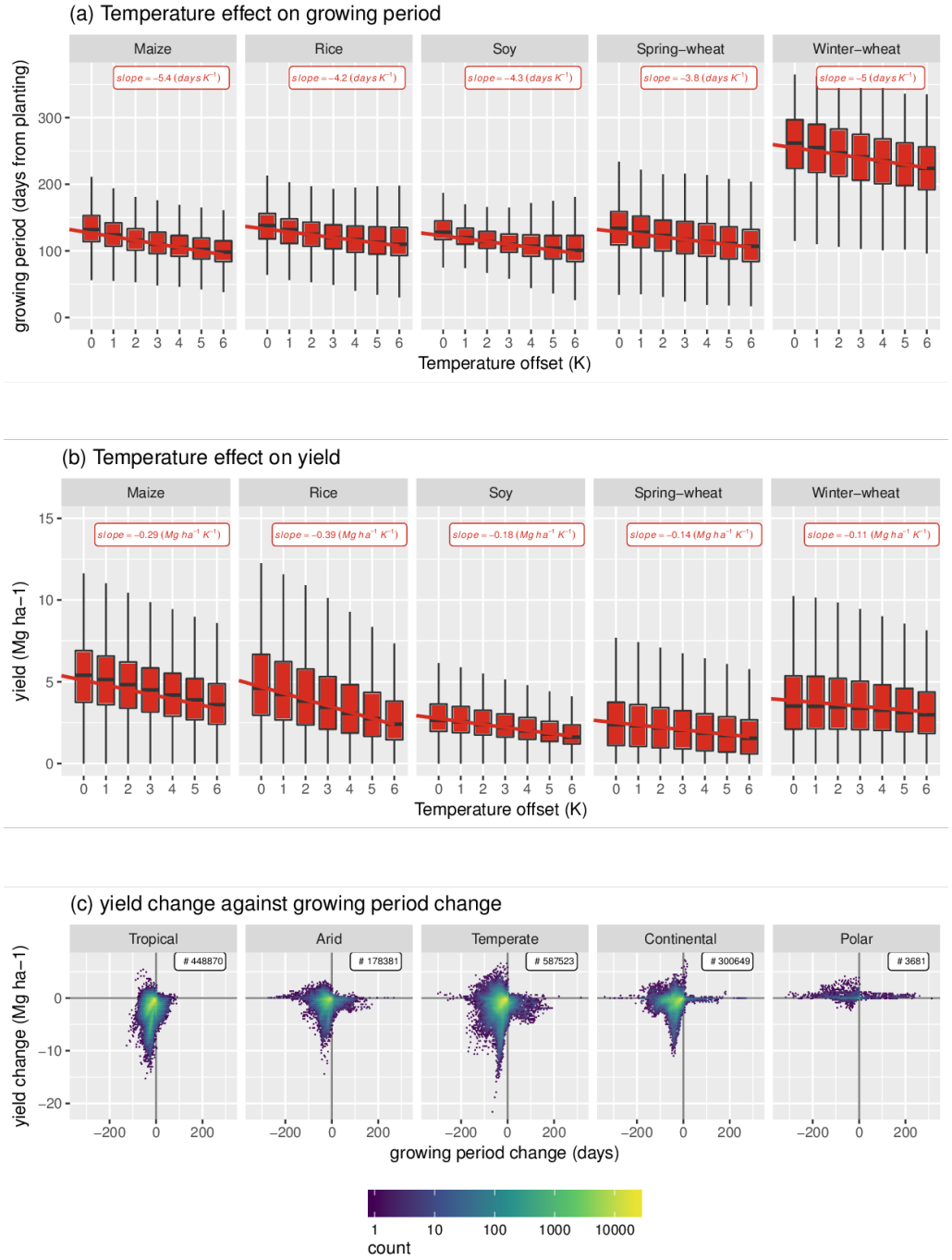

Figure 2: Effect of increasing temperature on crop phenology (growing period duration, days from planting) (a) and on yield (b) of the different rainfed crops. Each box represents the distribution of all grid cells values of all GGCMs for a specific temperature offset. Linear regression lines across all grid cells and GGCMs are plotted and lables report estimated intercept and slope. The heat map in panel (c) displays the relationship between yield changes (Mg ha^{-1}) and growing period changes (days) with increasing temperature. Changes are measured as differences between the values of the variable under a warmer and the reference temperature respecively. Each panel include all simulated grid cells at all temperature offsets between T1 and T6) of all crops in a climate region. Hexagons are colored according to their frequency count.

2.3 Effectiveness of adaptation measures

Increasing temperatures decrease global production of all crops almost linearly, except for winter-wheat, where decreases only start at a warming of ~ 2 K. Using different cultivars, so that the original growing period is maintained under warming (*fixed growing period* setting; yellow lines in Fig. 3), the total global calorie production of all five crops can be stabilized up to ~ 2 K and declines with further warming. This results from different temperature responses of the individual crops. Rice, soy and spring-wheat show an almost linear decline with warming. For maize, the *fixed growing period* setting leads to stable global maize production up to warming of ~ 3 K. For winter-wheat, warming of up to ~ 3 K is projected to even increase global production and decreases only occur after that warming level. At the global aggregation level, the different GGCMs agree very well on these responses patterns, with the greatest uncertainty for winter-wheat (yellow shaded area in Fig. 3). Converting all rainfed to irrigated cropland (assuming unlimited water supply; *irrigation* setting) would increase global calorie production by ~ 20% (blue lines in Fig. 3). However, also fully irrigated production would directly decline with increasing temperatures at similar rates as rainfed production. The intensification through irrigation would maintain current production levels up to ~ 4 K. Similar patterns are displayed by all crops, but winter-wheat could maintain current production levels up to the maximum warming level tested here (6 K). Across the different GGCMs, the effects of irrigation of currently rainfed cropland are generally more uncertain than the effects of warming on rainfed crop production. In combination, the *fixed growing period* and *irrigation* measures facilitate a positive response of global calorie production to warming up to 4 K (green line in Fig. 3). For all warming levels tested here, the combined effect of the *fixed growing period* and *irrigation* measures leads to increased global calorie production on current rainfed cropland. For maize, the combination of the *fixed growing period* and *irrigation* measures leads to continuous increases in production with warming. Current global rainfed rice production cannot be maintained even with the combination of the *fixed growing period* and *irrigation* beyond $2K$. The size of the response of spring-wheat production to introducing *irrigation* to all rainfed areas is highly uncertain across GGCMs, as two models (LPJmL and pDSSAT) project roughly doubled spring-wheat production under irrigation, whereas the other models often project increases of only 25%. However, the uniform decline of irrigated spring-wheat production on rainfed cropland is robust across all GGCMs.

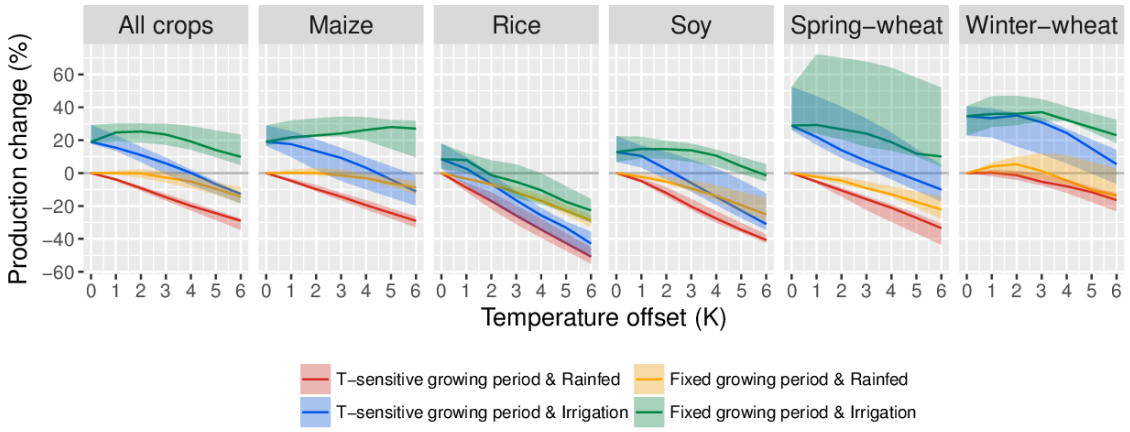

Figure 3: Impact (%) of increasing temperature and of four management settings on global calorie production of all crops aggregated as well as of each crop. The lines and the shaded area represent the median and the interquartile range (25^{th} to 75^{th} percentiles) of the GGCM ensemble respectively.

The effectiveness of the the *fixed growing period* adaptation differs across regions. In temperate and continental regions, there is greater potential for adaptation through the *fixed growing periods* than in tropical and arid regions. Fig. 4a shows the effectiveness of the *fixed growing period* adaptation for a warming level of 4 K, however, the patterns are very robust across all warming levels tested here (see Appendix Fig. S12). There are substantial differences in the global patterns of adaptation effectiveness across the GGCMs (Fig. 4b, S13). There is greater agreement on where *fixed growing period* has little adaptation effectiveness, but models often disagree (larger ensemble AI standard deviation) on the magnitudes of the adaptation effectiveness of the *fixed growing period* measure (Fig. 4b). The *fixed growing periods* measure has hardly any positive effect in arid regions, but has the potential to maintain current production levels in continental regions (see Appendix Fig. S12). In arid regions, the *fixed growing period* measure can lead to amplified damages and would thus be a form of "maladaptation" (Fig. 4a, S13, S14). In tropical regions, *irrigation* has little potential to intensify production, whereas it obviously has very large potential in arid regions if water was available for this (see Appendix Fig. S12).

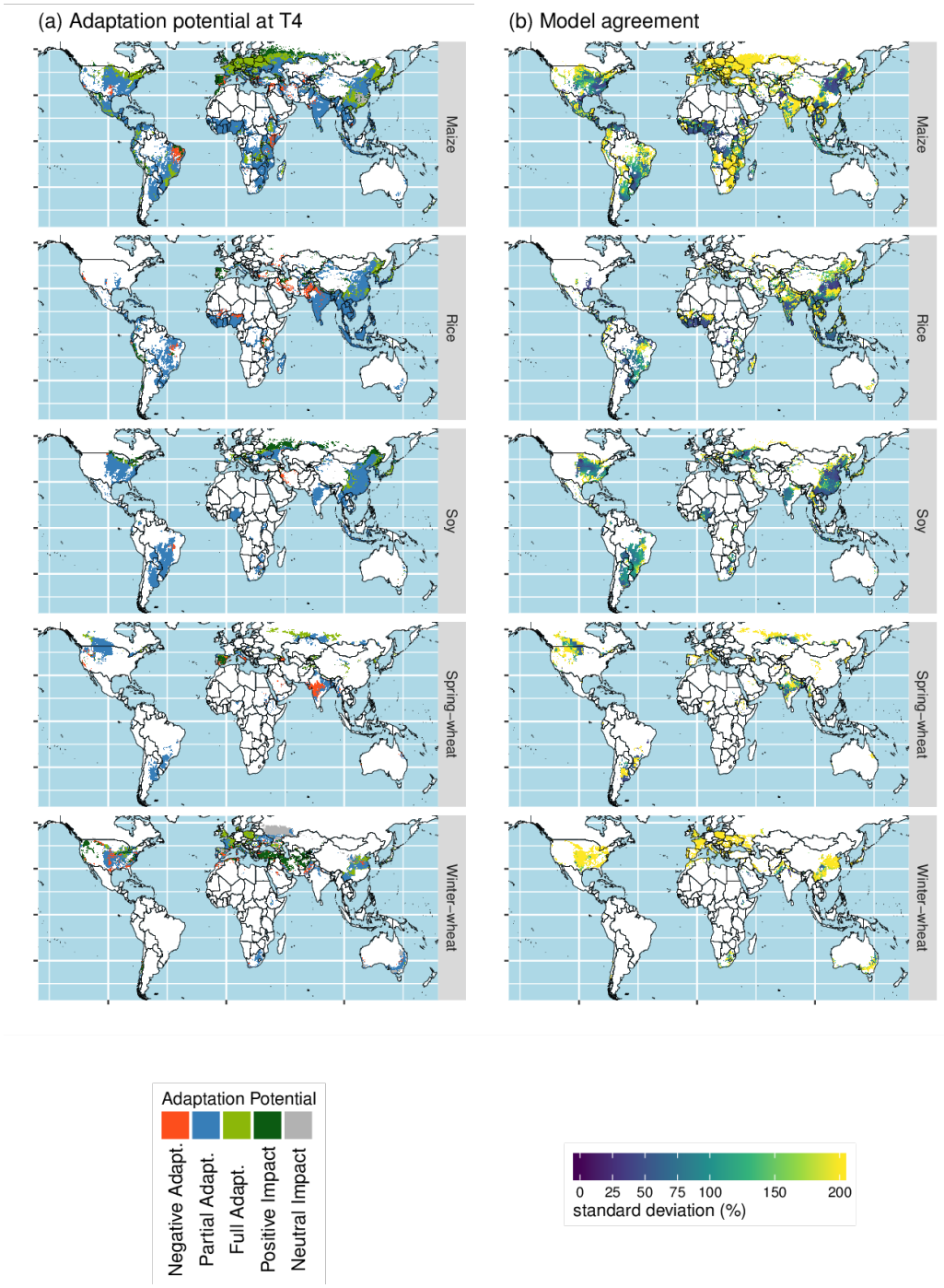

Figure 4: Impacts of temperature increase (a) and adaptation potential (AI) of rainfed crops with *fixed growing period* at 4 K of temperature increase. a and AI are computed as in Eq. 2. Panel (a) shows the areas where the GGCMs ensemble median estimates: (i) both negative temperature impact and negative adaptation effect (orange, $a < 0$ & $AI < 0$); (ii) negative temperature impact and positive adaptation effect, but with only partial compensations of yield losses (blue, $a < 0$ & $0 < AI < 100$); (iii) negative temperature impact and positive adaptation effect, with full compensation of yield losses (light green, $a < 0$ & $AI > 100$); (iv) positive temperature impacts (dark green, $a > 0$); (v) neutral impacts (gray, $a = 0$). Panel (b) shows 2 standard deviations of AI across GGCMs, only in the grid cells where temperature increase has negative impacts ($a < 0$).

3 Discussion

Using a large GGCM ensemble in a systematic warming experiment, we find that temperature increase leads to continuous reductions in global crop production, which is in line with previous findings (Challinor et al., 2014; Rosenzweig et al., 2014; Lobell et al., 2011; Liu et al., 2016; Zhao et al., 2017). Our results suggest that this decline is driven by a combination of accelerated phenology and thus shorter growing periods as well as by direct effects on plant growth. As such, selecting cultivars that maintain the original growing period under warming is a viable adaptation measure in most regions, as it reduces or fully compensates negative effects of warming on crop yields. The response is variable across regions, crops and GGCMs and thus subject to uncertainty.

In absence of information on crop and cultivar parameters, process-based model applied at the global scale have to make assumptions. Folberth et al. (2016) demonstrate how important the assumptions on management aspects are for simulating crop yields. As such, it can be expected that the same assumptions also affect the modeled effects of adaptation. Previous GGCM ensemble studies showed that harmonization of management settings (Elliott et al., 2015) can have substantial effects on model performance (Müller et al., 2017), however, only a small set of those can be harmonized with existing global data sets (e.g. fertilizer, growing periods). In this exercise, modelers were asked to parametrize crop phenology so that the current growing period is reproduced in the reference simulation (AgMERRA climate data, (Ruane et al., 2015)). In the simulations without *fixed growing period* adaptation (*T-sensitive growing period* setting), this parametrization was not changed so that the simulated growing period responds to warming, depending on the individual GGCMs' implementation of phenology modules (Tab. 1). In the *fixed growing period* adaptation setting, the crop phenology parameters were re-calibrated for each warming level, so that the growing season was roughly unaffected by warming. However, no harmonization was requested for any other cultivar parameters or the functional form of the phenological response to temperature (Tab. 1). As such, the ensemble of GGCMs used here reflects a broader variety of cultivars and management systems, which may explain part of the diverse modeled regional response to *fixed growing period* adaptation. Cardinal temperatures of phenological development are considered crop specific (Hatfield et al., 2011), with very little variability within species among genotypes and no acclimation to changes in temperature (Parent & Tardieu, 2012), therefore supporting the use by the GGCMs of crop-specific global parameters in the temperature response function for phenology. On the other hand, photosynthesis and enzyme activity acclimate to higher temperature (Parent & Tardieu, 2012) and cultivars differ for their sensitivity to heat stress. In particular, cultivars that are selected in hot climates are less sensitive to yield losses Butler & Huybers (2013), a feature that is not reflected in the GGCMs. Rezaei et al. (2018) suggest that the temperature response in phenology could be flawed by not accounting for changes in cultivar choice in the historic past. Also Zhu et al. (subm) find that GGCMs often overestimate the response in growing period length compared to other yield-reducing effects of warming. This uncertainty in regional responses is in contrast to the robust finding of *fixed growing period* adaptation at the global aggregation, where models do not differ much. It remains unclear how the diverse regional responses need to be aggregated. Considering the complex interaction of initial cultivar parameterization for baseline yields and warming effects (Folberth et al., 2016) this requires further research and requires better information on existing management systems globally.

Following the definition of Lobell (2014) for adaptation, we find that converting rainfed

crop production cannot be considered a true adaptation measure, but rather a measure of intensification. This is because the beneficial effect of this change in management has no greater benefit under warming than under current conditions. This is surprising to some extent, because previous studies find that irrigation reduces the direct negative effects of warming on crop yields. Schauberger et al. (2017) find that irrigation buffers against damages from exposure to hot temperatures for maize in the USA and maize yield response to temperature is found to be highly leveraged by soil moisture status (Carter et al., 2016) and thus presumably irrigation in dryer areas. The lack of reproducing this effect in this model ensemble may be due to several reasons. First, only one of the seven GGCMs (PROMET) accounts for the cooling effect of increased transpiration under irrigation by simulating canopy temperatures, whereas all other models assume canopy temperature to be equal to air temperatures. However, also PROMET shows the same pattern in the response to irrigation and warming as all the other GGCMs: intensification of production through converting rainfed to irrigated production, but no benefit on the negative response to warming (see Appendix Fig. S11). Second, if models tend to overestimate the growing period response to warming as suggested by Rezaei et al. (2018); Zhu et al. (subm), the shortening of the growing season may overly dominate the yield response and direct effects of warming on plant growth are underrepresented in the model results. If canopy temperatures are not accounted for, irrigation cannot affect the simulated length of the growing period and will not show in the underrepresented effects on crop growth. Nonetheless this intensification could compensate for much of the warming-induced damage, at least in regions where irrigation water could be supplied.

We find that the challenge to maintain current productivity levels under warming is particularly large in the tropical and arid climate zones, given that the adaptation of *fixed growing period* has little potential to reduce the negative effects of warming on crop yields and that shifting rainfed to irrigated production has little potential in the tropics and will be severely hampered by water availability in most arid regions. Also, the tropics are bound to experience climate conditions that have no analogues under current climate conditions (Pugh et al., 2016), so that breeding or designing cultivars for such conditions will be particularly challenging.

Generally, the GGCMI CTWN-A modeling experiment is an artificial setup with several implications for the interpretation of results (Franke et al., subm). Firstly, we here only study the effects of warming in a uniform manner, i.e. all days warm by exactly the same offset, which is not representative for realistic climate change scenarios. Second, associated impacts from changes in precipitation under climate change as well as elevated atmospheric CO_2 concentrations, which drive climate change (**?**) are ignored. These can often enhance (Kimball, 2016), but also reduce (Prasad et al., 2006) crop growth. Third, we here consider only high-input systems with nitrogen fertilization levels of $200 kg N ha^{-1}$ and no other nutrient limitations (e.g. P, K). However, we render these simplifications as justified, as we are aiming to understand how warming-induced damages to crop production can be compensated by an adaptation measure the counteracts the phenological acceleration, which is almost exclusively temperature driven. This artificial setup helps to isolate effects, which are typically difficult to separate in realistic climate scenarios, in which the relationship of changes in temperature, precipitation and atmospheric CO_2 concentrations are very model dependent (McSweeney & Jones, 2016). Still, results from the GGCMI CTWN-A experiment as analyzed here should not be misinterpreted as assessments of adaptation options under realistic climate change scenarios.

The adaptation measure to regain the warming-induced loss of growing period duration

considered here is also a simplified theoretical case. As the maintaining of the original growing period is not always beneficial or somewhat shorter or longer growing periods could have even greater potential to adapt to warming, this only represents one specific case of a broader continuum. Also, adaptation in cultivar choice is likely linked to changes in sowing dates to best adapt cropping systems to changed climatic conditions, which is especially relevant in regions with temperature seasonality (Waha et al., 2012). However, selecting a static growing season as a uniform adaptation measure again facilitates better interpretation of the results. Still, uncertainty are linked to the differences in interpreting the modeling protocol. The simulations conducted by CARAIB did not parametrize cultivar traits to reproduce the harmonization target for crop maturity (Elliott et al., 2015), but do keep their growing seasons constant under warming in the adaptation setup. Other models did follow the harmonization protocol, but growing seasons are not always closely reproduced (see Appendix Fig. S2). This contributes to the uncertainty in the modeled response to adaptation.

4 Conclusions

Future warming as projected under climate change will negatively affect crop production. Despite possibly compensating or amplifying effects form simultaneously changing precipitation and atmospheric CO_2 concentrations, it is important to understand options for adapting to the warming-induced yield reductions. Using a global gridded crop model ensemble, we find that adapting new cultivars that would maintain current crop growing periods under warming is a viable option with substantial potential to fully compensate warming-induced yield reductions, especially in the temperate and continental climate zones. Even though growing period adaptation also shows positive effects in the tropics, but hardly any in arid regions, these effects are insufficient to fully compensate warming-induced yield reduction even at low levels of warming. Tropical regions are also not very responsive to introducing irrigated production systems so that maintaining current crop productivity under warming is particularly challenging in the tropics. The lack of knowledge on current management systems at the global scale renders model simulations at this scale as particularly uncertain. Despite this uncertainty we find globally aggregated impacts and effects of adaptation to be robust across the model ensemble, that implicitly represents a broader set of management systems by differing in the parametrization of management-related features. Future research will have to exploit the potential for adaptation and intensification in temperate and continental climate zones to contribute to future food security and will have to identify ways how the double burden of strong climate change impacts and low adaptation potential in the tropical and arid climate zones can be alleviated.

4.1 Acknowledgments

...

References

Asseng, S., Zhu, Y., Wang, E., & Zhang, W. (2015). Crop modeling for climate change impact and adaptation. In *Crop Physiology (Second Edition)* (pp. 505–546). Elsevier.

Burke, M. & Emerick, K. (2016). Adaptation to climate change: Evidence from us agriculture. *American Economic Journal: Economic Policy*, *8*(3), 106–40.

Butler, E. E. & Huybers, P. (2013). Adaptation of us maize to temperature variations. *Nature Climate Change*, *3*(1), 68–72.

Carter, E. K., Melkonian, J., Riha, S. J., & Shaw, S. B. (2016). Separating heat stress from moisture stress: analyzing yield response to high temperature in irrigated maize. *Environmental Research Letters*, *11*(9), 094012.

Challinor, A. J., Watson, J., Lobell, D., Howden, S., Smith, D., & Chhetri, N. (2014). A meta-analysis of crop yield under climate change and adaptation. *Nature Climate Change*, *4*(4), 287.

Dowle, M. & Srinivasan, A. (2017). *data.table: Extension of 'data.frame'*. R package version 1.10.4-3.

Egli, D. B. (2011). Time and the productivity of agronomic crops and cropping systems. *Agronomy journal*, *103*(3), 743–750.

Elliott, J., Müller, C., Deryng, D., Chryssanthacopoulos, J., Boote, K., Büchner, M., Foster, I., Glotter, M., Heinke, J., Iizumi, T., et al. (2015). The global gridded crop model intercomparison: data and modeling protocols for phase 1 (v1. 0). *Geoscientific Model Development*, *8*(2), 261–277.

Eyshi Rezaei, E., Webber, H., Gaiser, T., Naab, J., & Ewert, F. (2015). Heat stress in cereals: Mechanisms and modelling. *European Journal of Agronomy*, *64*, 98–113.

FAO (2001). Food balance sheets a handbook. *Food and Agriculture Organization, Rome, Italy*.

Folberth, C., Elliott, J., Müller, C., Balkovic, J., Chryssanthacopoulos, J., Izaurralde, R. C., Jones, C., Khabarov, N., Liu, W., Reddy, A., et al. (2016). Uncertainties in global crop model frameworks: effects of cultivar distribution, crop management and soil handling on crop yield estimates. *Biogeosciences Discussions*, 1–30.

Franke, J., Elliott, J., Müller, C., Ruane, A., Snyderf, A., Jägermeyr, J., Balkovicg, J., Ciais, P., Dury, M., Falloon, P., Folberth, C., et al. (subm). The ggcmi phase ii experiment: global crop yield responses to changes in carbon dioxide, temperature, water, and nitrogen levels. *Agricultural and Forest Meteorology*.

Hatfield, J. L., Boote, K. J., Kimball, B., Ziska, L., Izaurralde, R. C., Ort, D., Thomson, A. M., & Wolfe, D. (2011). Climate impacts on agriculture: implications for crop production. *Agronomy journal*, *103*(2), 351–370.

Kimball, B. A. (2016). Crop responses to elevated co2 and interactions with h2o, n, and temperature. *Current opinion in plant biology*, *31*, 36–43.

Liu, B., Asseng, S., Müller, C., Ewert, F., Elliott, J., Lobell, D. B., Martre, P., Ruane, A. C., Wallach, D., Jones, J. W., et al. (2016). Similar estimates of temperature impacts on global wheat yield by three independent methods. *Nature Climate Change*, *6*(12), 1130.

Lobell, D. B. (2014). Climate change adaptation in crop production: Beware of illusions. *Global Food Security*, *3*(2), 72–76.

Lobell, D. B., Schlenker, W., & Costa-Roberts, J. (2011). Climate Trends and Global Crop Production Since 1980. *Science*, *333*(6042), 616–620.

McSweeney, C. F. & Jones, R. G. (2016). How representative is the spread of climate projections from the 5 cmip5 gcms used in isi-mip? *Climate Services*, *1*, 24–29.

Müller, C., Elliott, J., Chryssanthacopoulos, J., Arneth, A., Balkovic, J., Ciais, P., Deryng, D., Folberth, C., Glotter, M., Hoek, S., et al. (2017). Global gridded crop model evaluation: benchmarking, skills, deficiencies and implications. *Geoscientific Model Development Discussions*, *10*, 1403–1422.

Parent, B., Leclere, M., Lacube, S., Semenov, M. A., Welcker, C., Martre, P., & Tardieu, F. (2018). Maize yields over europe may increase in spite of climate change, with an appropriate use of the genetic variability of flowering time. *Proceedings of the National Academy of Sciences*, *115*(42), 10642–10647.

Parent, B. & Tardieu, F. (2012). Temperature responses of developmental processes have not been affected by breeding in different ecological areas for 17 crop species. *New Phytologist*, *194*(3), 760–774.

Parent, B., Turc, O., Gibon, Y., Stitt, M., & Tardieu, F. (2010). Modelling temperature-compensated physiological rates, based on the co-ordination of responses to temperature of developmental processes. *Journal of Experimental Botany*, *61*(8), 2057–2069.

Pierce, D. (2015). *ncdf4: Interface to Unidata netCDF (Version 4 or Earlier) Format Data Files*. R package version 1.15.

Portmann, F. T., Siebert, S., & Döll, P. (2010). Mirca2000—global monthly irrigated and rainfed crop areas around the year 2000: A new high-resolution data set for agricultural and hydrological modeling. *Global Biogeochemical Cycles*, *24*(1).

Prasad, P. V., Boote, K. J., & Allen Jr, L. H. (2006). Adverse high temperature effects on pollen viability, seed-set, seed yield and harvest index of grain-sorghum [sorghum bicolor (l.) moench] are more severe at elevated carbon dioxide due to higher tissue temperatures. *Agricultural and forest meteorology*, *139*(3-4), 237–251.

Pugh, T. A., Müller, C., Elliott, J., Deryng, D., Folberth, C., Olin, S., Schmid, E., & Arneth, A. (2016). Climate analogues suggest limited potential for intensification of production on current croplands under climate change. *Nature Communications*, *7*, 1–8.

R Core Team (2018). *R: A Language and Environment for Statistical Computing*. Vienna, Austria: R Foundation for Statistical Computing.

Rezaei, E. E., Siebert, S., Hüging, H., & Ewert, F. (2018). Climate change effect on wheat phenology depends on cultivar change. *Scientific reports*, *8*(1), 4891.

Rosenzweig, C., Elliott, J., Deryng, D., Ruane, A. C., Müller, C., Arneth, A., Boote, K. J., Folberth, C., Glotter, M., Khabarov, N., et al. (2014). Assessing agricultural risks of climate change in the 21st century in a global gridded crop model intercomparison. *Proceedings of the National Academy of Sciences*, *111*(9), 3268–3273.

Rosenzweig, C., Jones, J. W., Hatfield, J. L., Ruane, A. C., Boote, K. J., Thorburn, P., Antle, J. M., Nelson, G. C., Porter, C., Janssen, S., et al. (2013). The agricultural model intercomparison and improvement project (agmip): protocols and pilot studies. *Agricultural and Forest Meteorology*, *170*, 166–182.

Rosenzweig, C., Ruane, A. C., Antle, J., Elliott, J., Ashfaq, M., Chatta, A. A., Ewert, F., Folberth, C., Hathie, I., Havlik, P., et al. (2018). Coordinating agmip data and models across global and regional scales for 1.5° c and 2.0° c assessments. *Phil. Trans. R. Soc. A*, *376*(2119), 20160455.

Ruane, A. C., Goldberg, R., & Chryssanthacopoulos, J. (2015). Climate forcing datasets for agricultural modeling: Merged products for gap-filling and historical climate series estimation. *Agricultural and Forest Meteorology*, *200*, 233–248.

Ruiz-Ramos, M., Ferrise, R., Rodríguez, A., Lorite, I., Bindi, M., Carter, T. R., Fronzek, S., Palosuo, T., Pirttioja, N., Baranowski, P., et al. (2018). Adaptation response surfaces for managing wheat under perturbed climate and co2 in a mediterranean environment. *Agricultural Systems*, *159*, 260–274.

Sacks, W. J., Deryng, D., Foley, J. A., & Ramankutty, N. (2010). Crop planting dates: an analysis of global patterns. *Global Ecology and Biogeography*, *19*(5), 607–620.

Schauberger, B., Archontoulis, S., Arneth, A., Balkovic, J., Ciais, P., Deryng, D., Elliott, J., Folberth, C., Khabarov, N., Müller, C., et al. (2017). Consistent negative response of us crops to high temperatures in observations and crop models. *Nature communications*, *8*, 13931.

Schleussner, C.-F., Deryng, D., Müller, C., Elliott, J., Saeed, F., Folberth, C., Liu, W., Wang, X., Pugh, T. A., Thiery, W., et al. (2018). Crop productivity changes in 1.5 c and 2 c worlds under climate sensitivity uncertainty. *Environmental Research Letters*, *13*(6), 064007.

Semenov, M., Stratonovitch, P., Alghabari, F., & Gooding, M. (2014). Adapting wheat in europe for climate change. *Journal of Cereal Science*, *59*(3), 245–256.

Waha, K., Van Bussel, L., Müller, C., & Bondeau, A. (2012). Climate-driven simulation of global crop sowing dates. *Global Ecology and Biogeography*, *21*(2), 247–259.

Wang, E., Martre, P., Zhao, Z., Ewert, F., Maiorano, A., Rötter, R. P., Kimball, B. A., Ottman, M. J., Wall, G. W., White, J. W., et al. (2017). The uncertainty of crop yield projections is reduced by improved temperature response functions. *Nature plants*, *3*(8), 17102.

Weedon, G. P., Balsamo, G., Bellouin, N., Gomes, S., Best, M. J., & Viterbo, P. (2014). The wfdei meteorological forcing data set: Watch forcing data methodology applied to era-interim reanalysis data. *Water Resources Research*, *50*(9), 7505–7514.

Wickham, H. (2009). *ggplot2: Elegant Graphics for Data Analysis*. Springer-Verlag New York.

Wickham, H. (2011). The split-apply-combine strategy for data analysis. *Journal of Statistical Software*, *40*(1), 1–29.

Wirsenius, S. (2000). *Human use of land and organic materials: modeling the turnover of biomass in the global food system*. Chalmers University of Technology.

Zhao, C., Liu, B., Piao, S., Wang, X., Lobell, D. B., Huang, Y., Huang, M., Yao, Y., Bassu, S., Ciais, P., Durand, J.-L., Elliott, J., Ewert, F., Janssens, I. A., Li, T., Lin, E., Liu, Q., Martre, P., Müller, C., Peng, S., Peñuelas, J., Ruane, A. C., Wallach, D., Wang, T., Wu, D., Liu, Z., Zhu, Y., Zhu, Z., & Asseng, S. (2017). Temperature increase reduces global yields of major crops in four independent estimates. *Proceedings of the National Academy of Sciences*, 201701762.

Zhu, P., Zhuang, Q., Archontoulis, S. V., Bernacchi, C., & Müller, C. (subm). Dissecting the nonlinear response of maize yield to high temperature stress with model-data integration. *Global Change Biology*.

5 Supplementary materials

5.1 GGCMI phase 2 CTWN-A protocol

The overall scientific rational of the GGCMI phase 2 protocol is to conduct a comparative analysis of the strategies and mechanisms used in different models to describe CTWN processes, interactions, and feedbacks. This analysis framework builds on the AgMIP Coordinated Climate-Crop Modeling Project [(Ruane et al., 2013; McDermid et al., 2015)] efforts to compare models, sites, and uncertainty and extends the concept now to global gridded simulations. This also provides a basis for comparison between grids and site-based networks. Moreover, it aims at enhanced understanding of how models work, characterizing models by sensitivity to drivers, and assess aggregated model responses at different aggregation levels (e.g. Köppn-Geiger climate zones).

GGCMI participants run models globally using harmonized input data. The AgMERRA climate data set from 1980-2010 is used as in phase 1 (Elliott et al., 2015). Groups that require data on long-wave radiation are asked to use the data from the Princeton GF (version 1, not PGFv2). Nitrogen and CO_2 are specified at globally uniform levels and will not be provided as spatially explicit data sets. Nitrogen fertilizer is to be applied in 2 doses, 50% at planting and 50% at a crop- and pixel specific date (40 days after planting for all spring crops, case-specific for winter wheat). All other sources of nitrogen supply (mineralization, fixation by soy) have to be reported in the outputs, no deposition or soil-only fixation should be applied. Modelers are asked to find implement themselves scenarios of CTWN offsets.

Four levels of participation are defined (*low, mid, high, super tier*). GGCM crop-specific output variables of highest priority have to be submitted per growing season: yield (t DM ha^{-1} yr^{-1}); total above ground biomass yield (t DM ha^{-1} yr^{-1}); actual planting date (day of year); anthesis date (day of year), maturity date (days from planting); applied irrigation water (mm yr^{-1}), evapotranspiration (growing season sum, mm yr^{-1}).

To reduce the computational burden, regions that are considered unsuitable are cut out of the simulation. Unsuitable areas are defined according to AEZ. There are a few cases, where (at the resolution of 0.5 degrees) the pixels is classified as dominantly unsuitable but the cropland masks assign cropland to these pixels. To ensure that all cropland currently used in the aggregation is also simulated by the groups, only pixels that are predominantly unsuitable (>=90%) and do not contain any cropland (according to MIRCA2000) are excluded. By excluding 'out-of-question areas', simulation results (all crops everywhere) can be aggregated by any land-use pattern in subsequent analyses.

5.2 Model characteristics and protocol implementation details

5.2.1 CARAIB

CARAIB simulates the crop development from sowing to harvest, requiring a certain (crop-specific) heat accumulation to be reached. A cultivar is attributed to each grid cell as a function of the cell growing season temperature and soil water availability (see below). To germinate a crop needs to accumulate some temperature and soil water conditions must also be suitable for seed germination, so that some delay can occur between sowing and germination. For instance, with a base temperature of $0°C$, wheat germinates when GDD0 = $140°Cd$ and only if soil water conditions are suitable. Wheat reaches maturity when GDD0 attains at least $1800°Cd$ but some cultivars require more (up to $4000°Cd$). In the

model, stress occurs under critical soil water content and (minimum) temperature.

CARAIB follows a modified protocol with harmonized sowing dates, while the model was not calibrated to match observed maturity dates of each grid cell. The simulated growing season of a crop is constrained by observed cropping calendars. Specifically, Sacks et al. (2010) is used to define the crop-specific maximum growing season length. For instance, if wheat does not reach maturity within 200 days, it is not harvested. Minimum and maximum GDD sums (extreme cultivars) are derived from observed growing period lengths, reported for each crop by Sacks et al. (2010). Between these extreme cultivars, there are a series of intermediate cultivars. A cultivar is attributed to each grid cell as a function of the cell temperature over the growing period (temperature accumulation) with soil water availability limiting the growing period length. The new-cultivar adaptation measure was implemented based on the partially-harmonized growing period length obtained under the baseline temperature scenario (T0). Adaptation was based on temperature only, while water limitations were kept constant under the rainfed as well as the irrigated scenarios.

5.2.2 GEPIC

GEPIC simulates the phenological development rate as null below T_{min}, equal to $T_{day} - T_{min}$ between T_{min} and T_{opt}, and maximum at T_{opt}.

To harmonize the growing periods growing degree days only were tuned. Default parameters from EPICv0810 for T_{min} and T_{opt} were used. T_{min} and T_{opt} together with long-term (1980-2010) monthly climate data were used to calculate the average GDD in each pixel based on reported harvest and planting dates.

GEPIC provided simulation results for a subset of T levels. The output variables of the missing levels (either T1 & T3, or T2) were derived by linear interpolation.

5.2.3 LPJ-GUESS

LPJ-GUESS simulates the phenological development rate as null below T_{min} and above T_{max}, and maximum at T_{opt}.

To harmonize the growing period GDD (PHUs) only were tuned.

LPJ-GUESS provided simulation results for a subset of crops: maize, spring-wheat, winter-wheat.

5.2.4 LPJmL

LPJmL simulates the phenological development rate as null below T_{min}, otherwise it is $T_{day} - T_{min}$.

To harmonize the growing periods GDD only were tuned. Simulations with increased GDD requirements were conducted, so that crops would grow beyond the prescribed harvest day and recorded the GDD accumulated on that day. For the CTWN-A simulations, the recorded GDD on the harvest day was averaged over the AgMERRA time period and prescribed per pixel and crop. Prescribed sowing dates are exactly met, prescribed maturity dates are met on average. Vernalization in winter-wheat made GDD pre-computation more complicated and maturity dates may be less accurate there.

5.2.5 pDSSAT

5.2.6 PEPIC

PEPIC simulates the phenological development rate as null below T_{min} and maximum at T_{opt} (default values of the EPIC model).

To harmonize the growing periods GDD only were tuned.

PEPIC provided simulation results for a subset of T levels. The output variables of the missing levels (either T1 & T3, or T2) were derived by linear interpolation.

5.2.7 PROMET

To simulate the crop phenological progress, PROMET uses a curvilinear (bell-shaped) temperature response function of crop development rate. Three parameters (T_{min}, T_{opt}, T_{max}) are used for calibrating the function: the rate is null below T_{min} and above T_{max}, and is maximum at T_{opt}. In addition, vernalization and light effect potentially inhibit phenological progress. Water stress is considered indirectly via the leaf temperature. PROMET uses leaf temperature, which leads to different phenology between rainfed and irrigated crops and all W-dimensions, because reduced water supply results in increased leaf temperatures that usually accelerates phenological development, but could also decrease phenological development rates, if temperature is already beyond the cardinal temperature of T_{opt}.

To harmonize the growing periods, sowing date were prescribed from the give data set and the model harvest date were pre-calculated. The offset between simulated harvest date and given harvest date were used to calibrate a phenological acceleration/retardation factor. Then the model was run again, this time matching the given dates for sowing and harvest. On some grid cells, the pre-calculation did not succeed, e.g. due to crop failure. In this case, no phenological acceleration/retardation factor could be calculated. These grid cells were masked out and yield is set to NA.

PROMET used ERAI as climate forcing dataset, because it has three-hourly simulation time step. PROMET outputs report yield failures as NA. We post-process yield data to fulfill reporting convention. We replaced all NA with 0 t ha-1 for yields in grids with MIRCA reported harvested area.

5.3 Supplementary tables

GGCM	Param.	maize	rice	soy	spring-wheat	winter-wheat
CARAIB	Tmin	8	8	7	0	0
	Topt	NA	NA	NA	NA	NA
	Tmax	NA	NA	NA	NA	NA
	GDDmin	1000	1000	1500	1800	2000
	GDDmax	3000	4000	3600	4000	4000
GEPIC	Tmin	8	10	10	5	0
	Topt	25	25	25	20	15
	Tmax	NA	NA	NA	NA	NA
	GDDmin	200	200	200	200	200
	GDDmax	4280	3728	3227	5291	6180
LPJ-GUESS	Tmin	8	NA	NA	0 - 8	0 - 8
	Topt	NA	NA	NA	24 - 29	24 - 29
	Tmax	NA	NA	NA	35 - 40	35 - 40
	GDDmin	100 (100)	NA	NA	209 (100)	342 (100)
	GDDmax	4210 (5059)	NA	NA	4600 (5768)	4600 (5791)
LPJmL	Tmin	5	10	10	0	0
	Topt	NA	NA	NA	NA	NA
	Tmax	NA	NA	NA	NA	NA
	GDDmin	700	700	700	700	700
	GDDmax	unlimited	unlimited	unlimited	unlimited	unlimited
pDSSAT	Tmin					
	Topt					
	Tmax					
	GDDmin					
	GDDmax					
PEPIC	Tmin	8	10	10	5	0
	Topt	25	25	25	20	15
	Tmax	NA	NA	NA	NA	NA
	GDDmin	unlimited	unlimited	unlimited	unlimited	unlimited
	GDDmax	unlimited	unlimited	unlimited	unlimited	unlimited
PROMET	Tmin	8	12-15	15-17	0	0 - 8
	Topt	30	22-28	24-26	25	19-24
	Tmax	42	40	40	37	30-35
	GDDmin	NA	NA	NA	NA	NA
	GDDmax	NA	NA	NA	NA	NA

Table S1: GGCMs phenology parametrization.

5.4 Supplementary figures

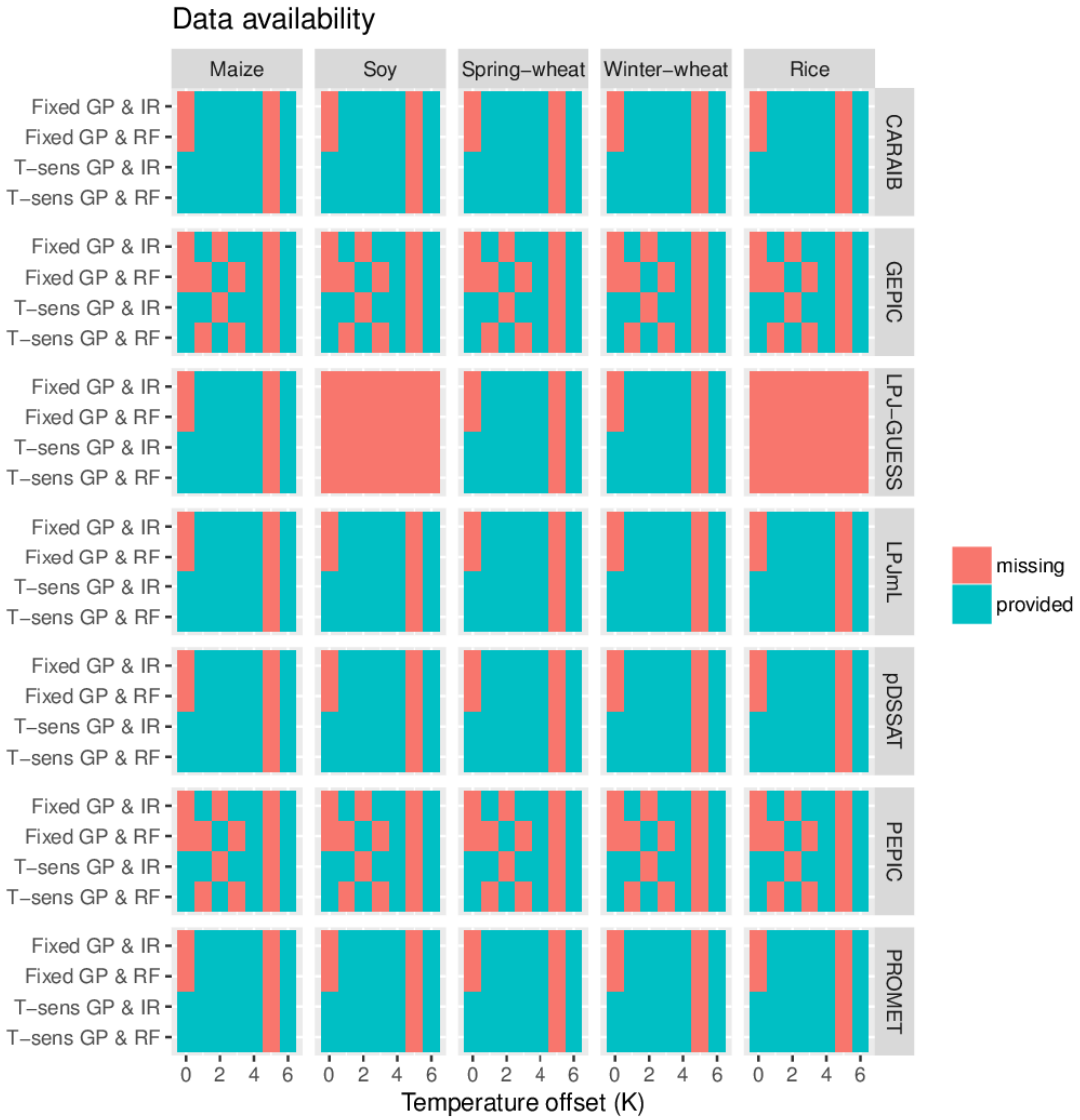

Figure S1: Available crop model simulations for each model, crop, temperature offset and management setting used in this study. Simulation setups missing (except for LPJ-GUESS rice and LPJ-GUESS soy) are interpolated as described in Section 1.1.2.

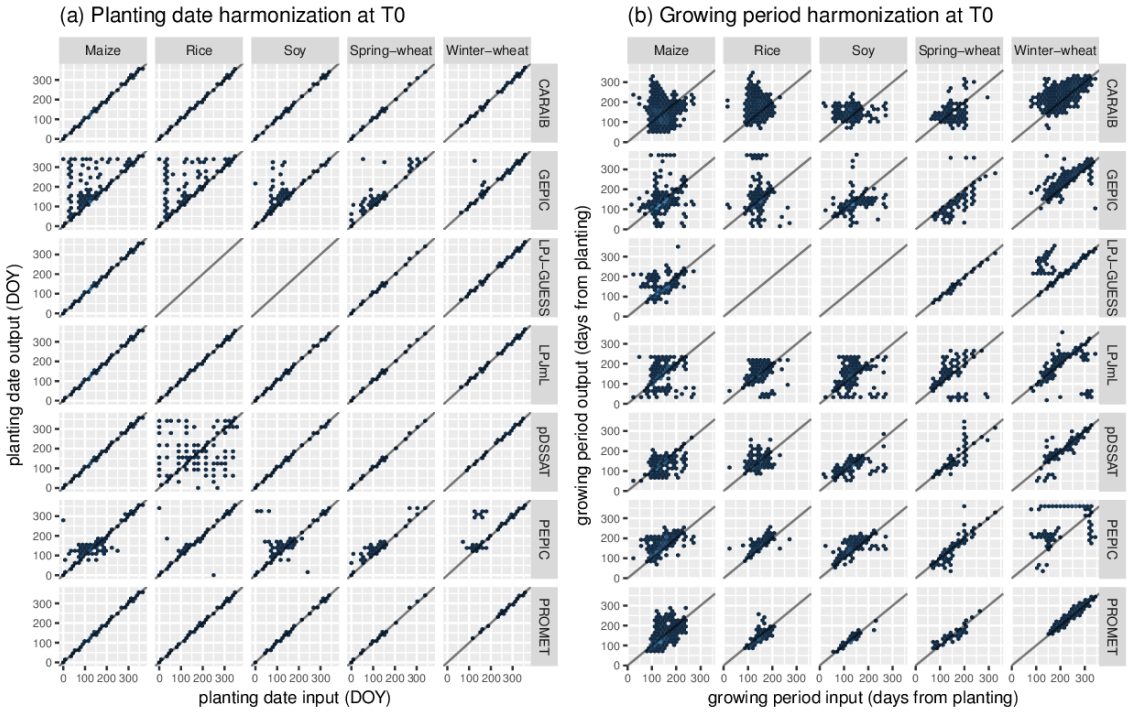

Figure S2: Evaluation of the growing period harmonization across GGCMs (T0, *historical management* setting). Prescribed planting (a) and maturity (b) dates are plotted against realized dated in each model (rows) and for each crop (column). The grey line is the 1:1 line. Across the model ensemble and crops 94% of the cultivated cells have a modeled planting date within ±3 days compared to the prescribed dates, CARAIB, LPJ-GUESS, LPJmL and PROMET for instance meets these dates in all cells, while others like PEPIC, GEPIC or pDSSAT, have large systematic errors for some of the crops and do not meet these dates in up to 44% of the cells. Across the model ensemble and crops only 40% of the cultivated cells have a modeled maturity date within ±3 days, and four models (CARAIB, PEPIC, PROMET, LPJmL) out of seven have maturity dates deviations larger than ±14 days from the observed in 22% or more of the cells.

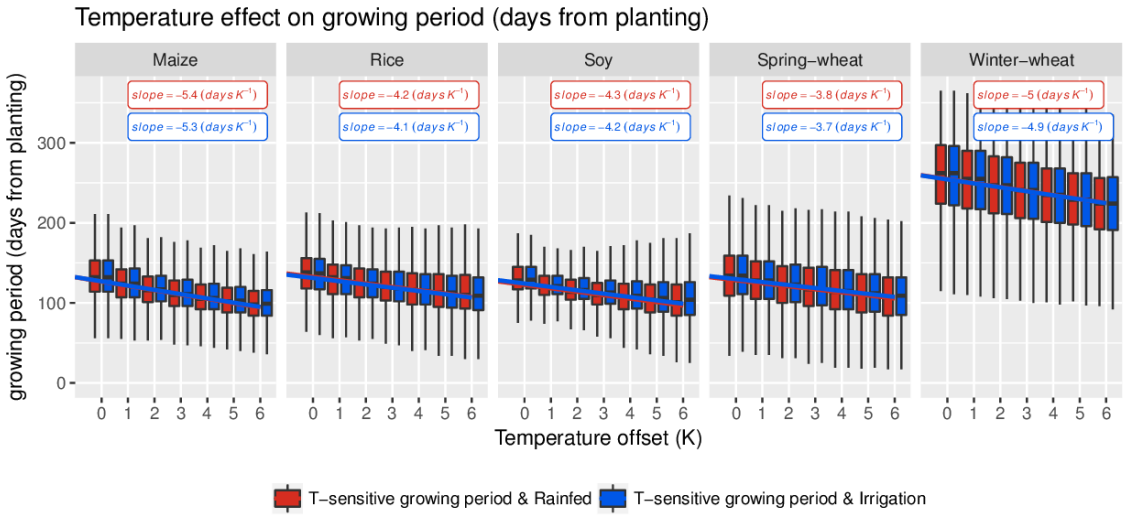

Figure S3: As Figure 2a but for both rainfed and irrited crops.

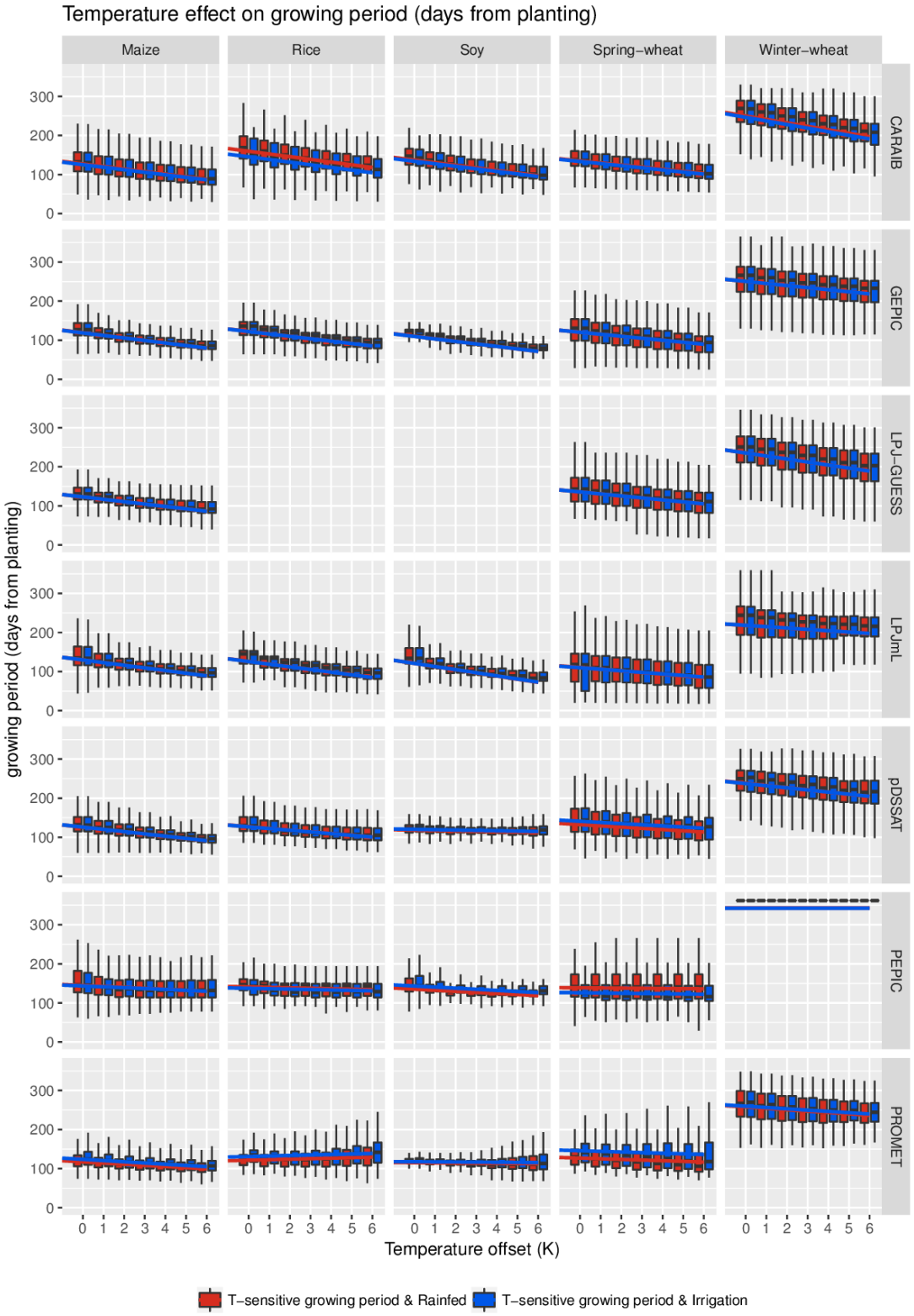

Figure S4: As Figure 2a but for both rainfed and irrited crops for each GGCM.

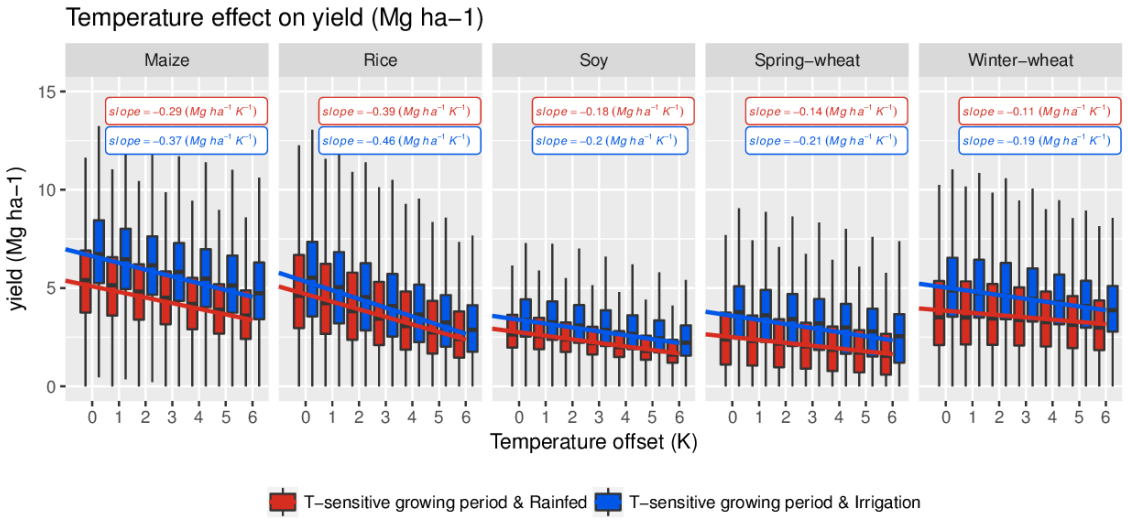

Figure S5: As Figure 2b but for both rainfed and irrited crops.

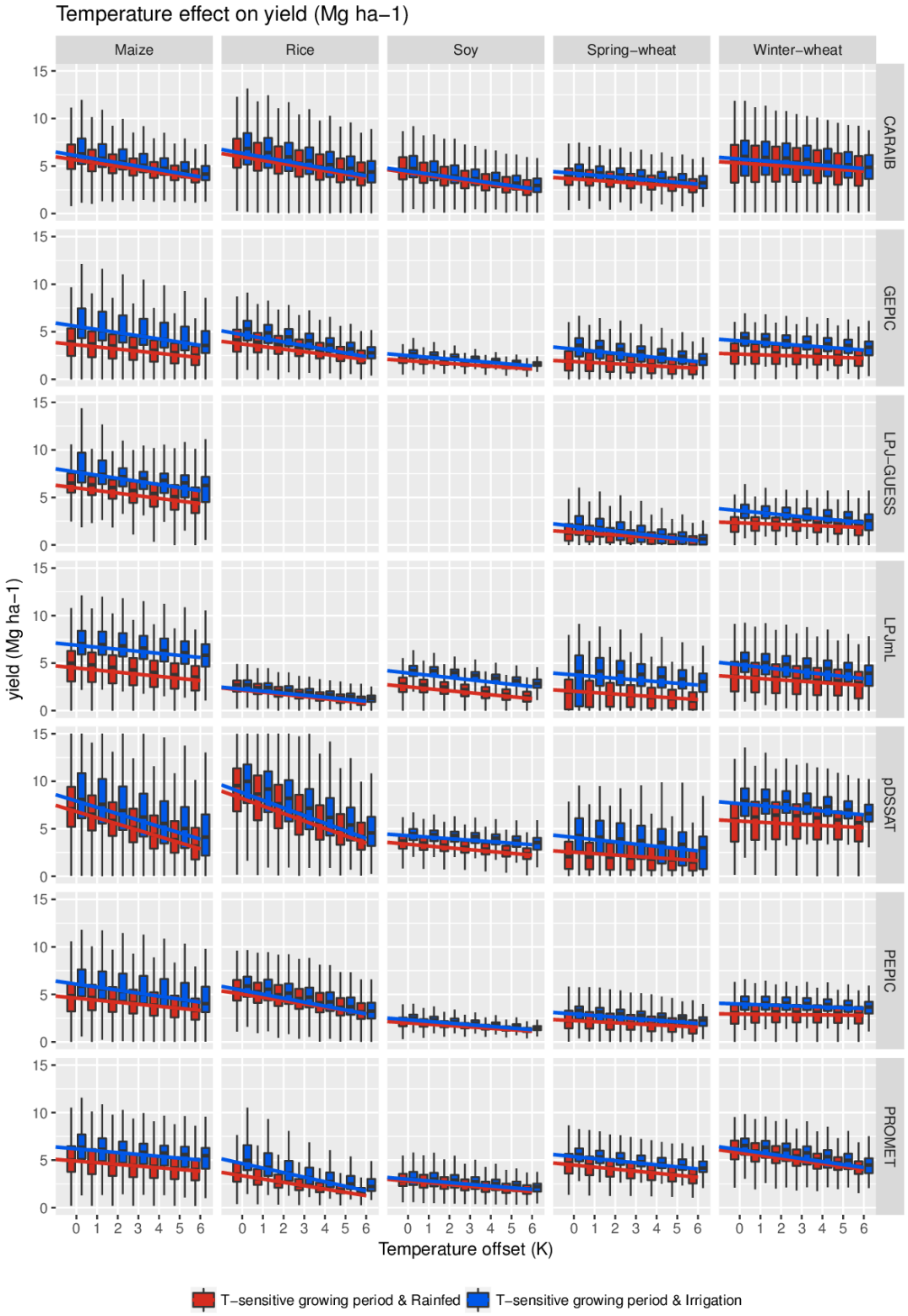

Figure S6: As Figure 2b but for both rainfed and irrited crops for each GGCM.

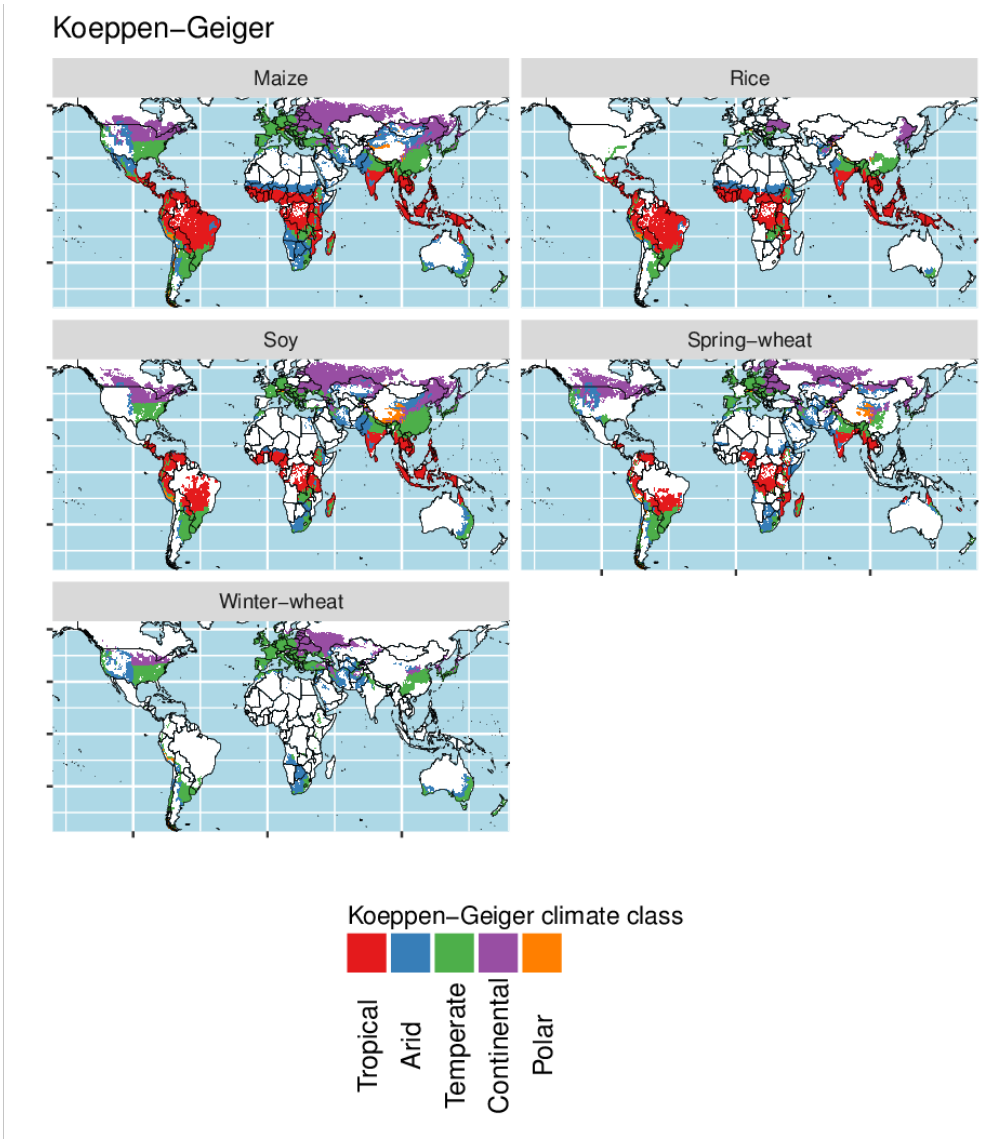

Figure S7: Cropland allocation in specific Koeppen-Geiger climate zones.

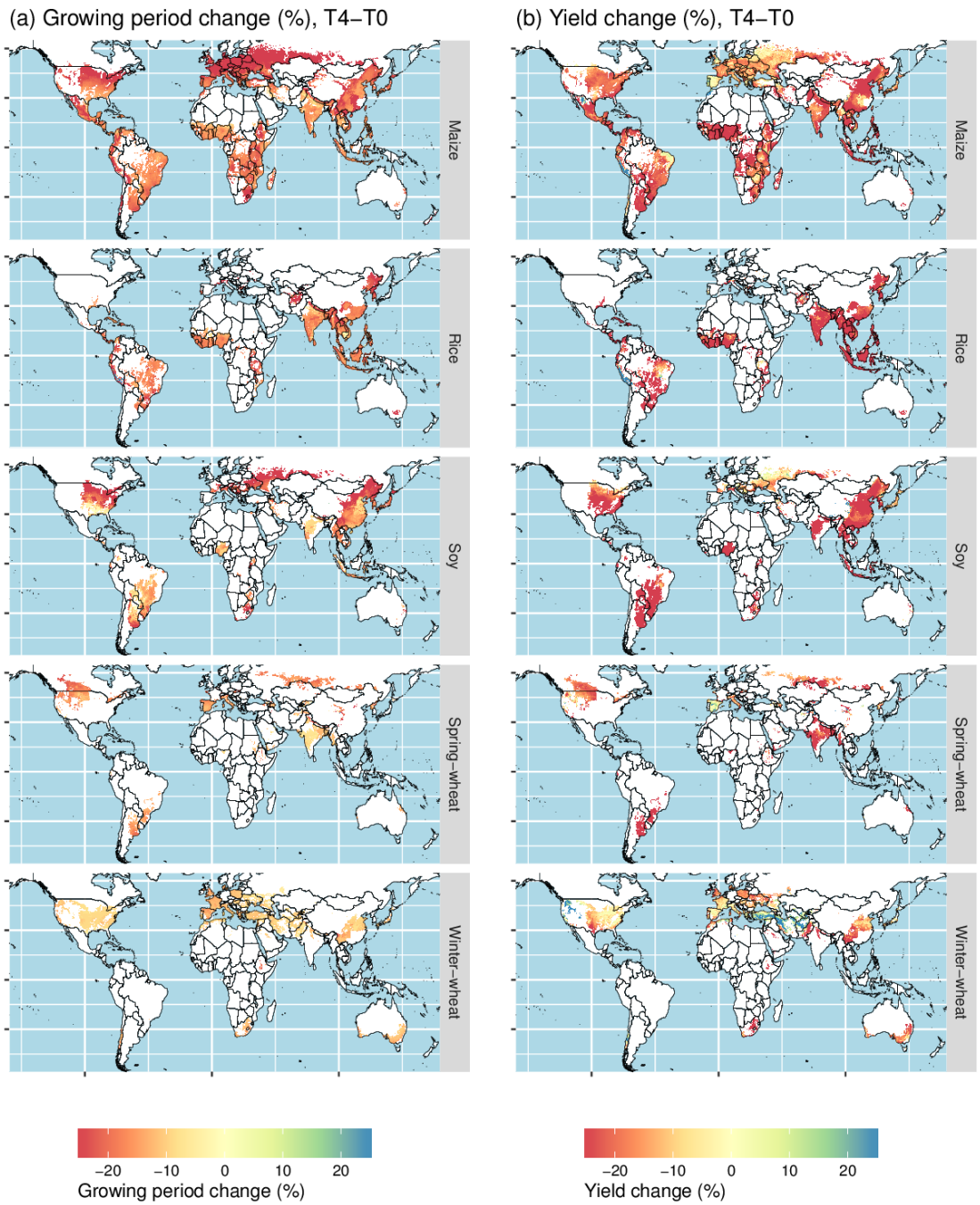

Figure S8: (a) Growing period change (%) and (b) yield change (%) with $4K$ temperature increase. Each panel shows crop-specific ensemble median of the difference T4-T0 under static management (CV_{old} + RF).

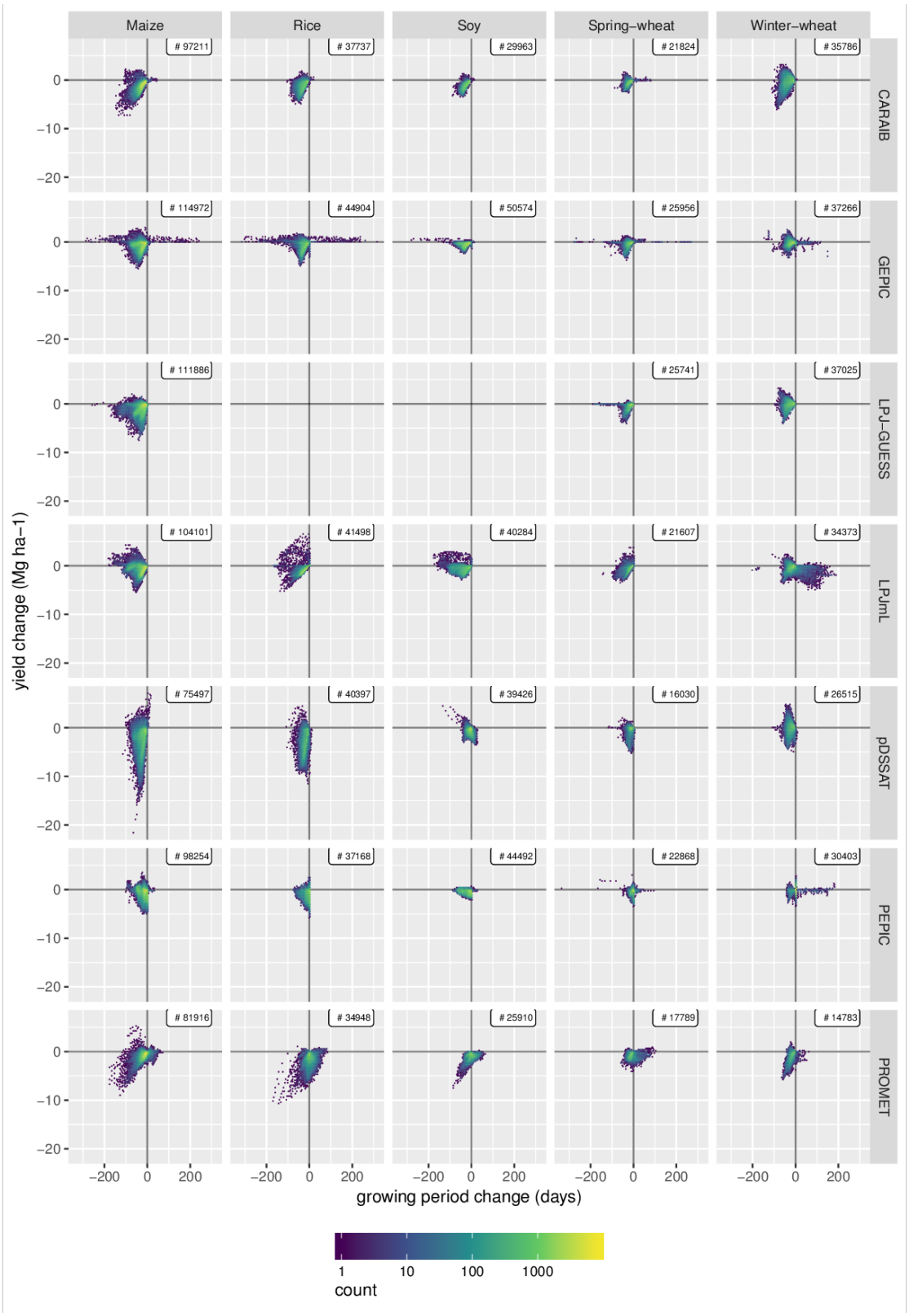

Figure S9: As Figure **??**c but for both rainfed and irrited crops for each GGCM.

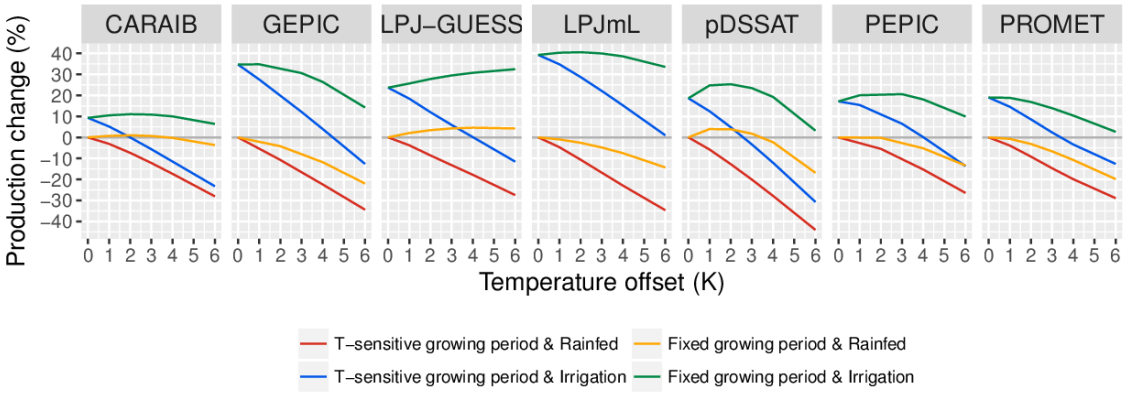

Figure S10: As Figure 3 (All crops), but for each GGCM.

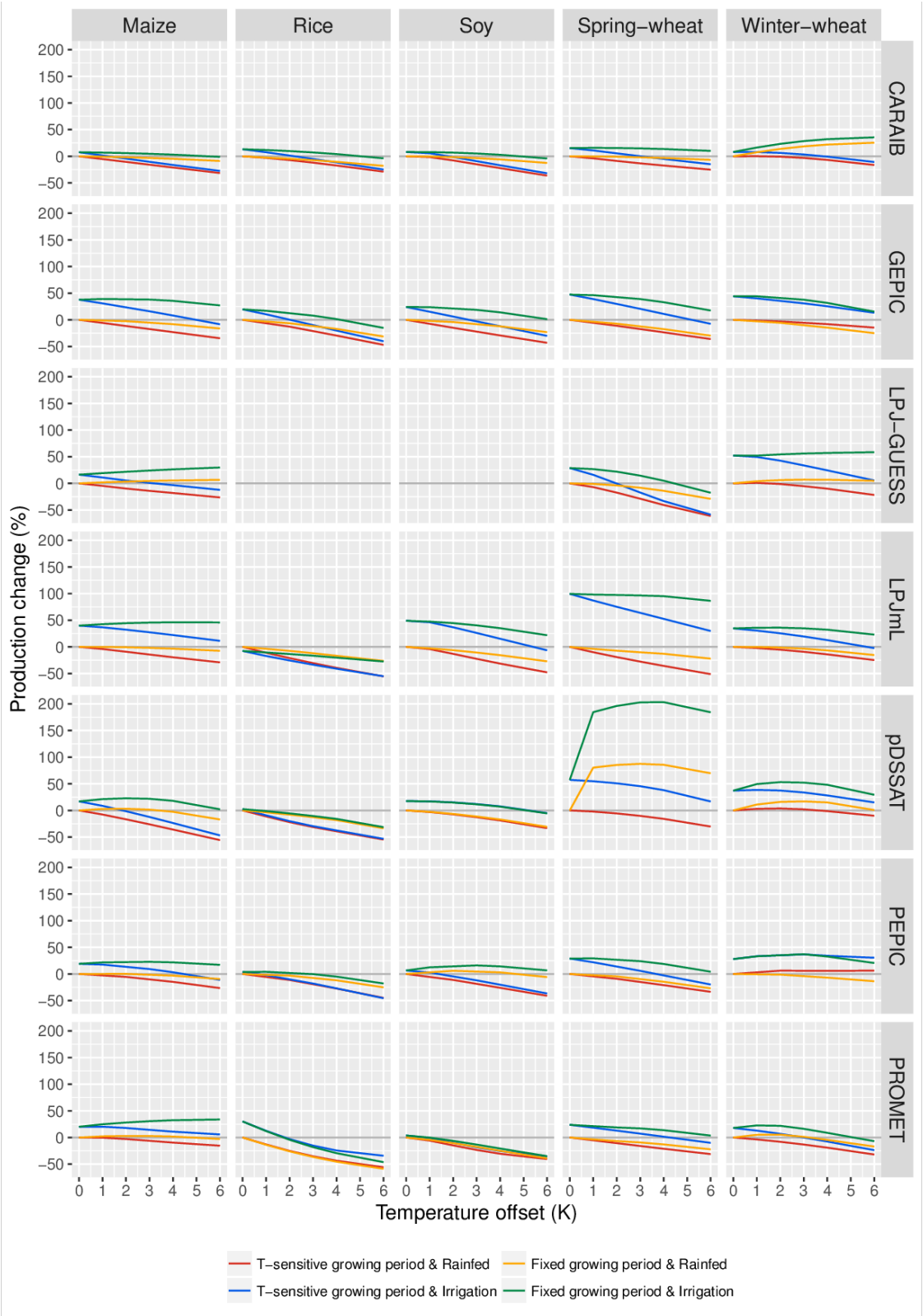

Figure S11: As Figure 3 but for each GGCM.

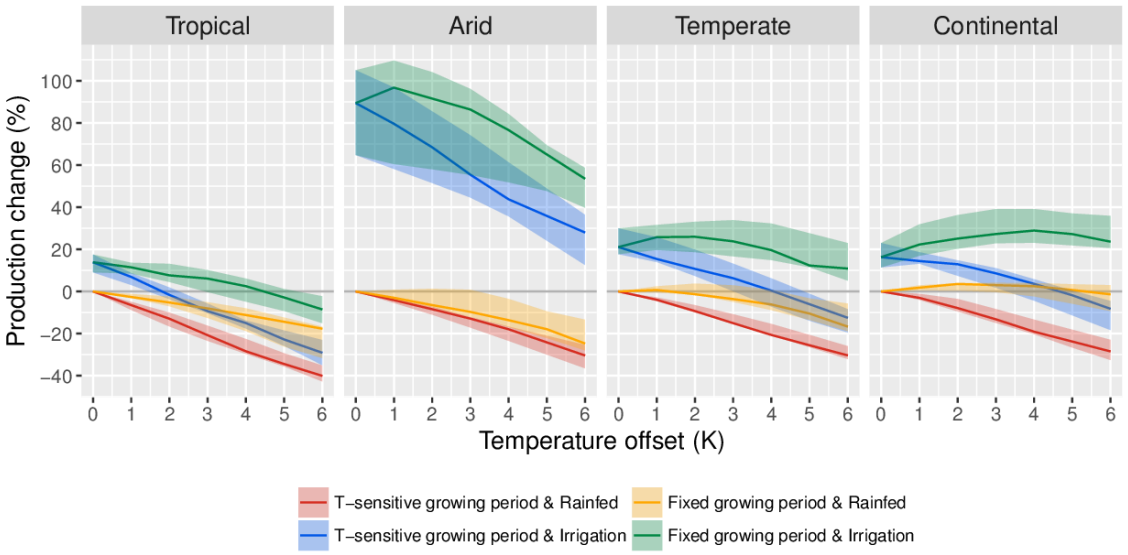

Figure S12: As Figure 3a, but for the Köppen-Geiger climate zones.

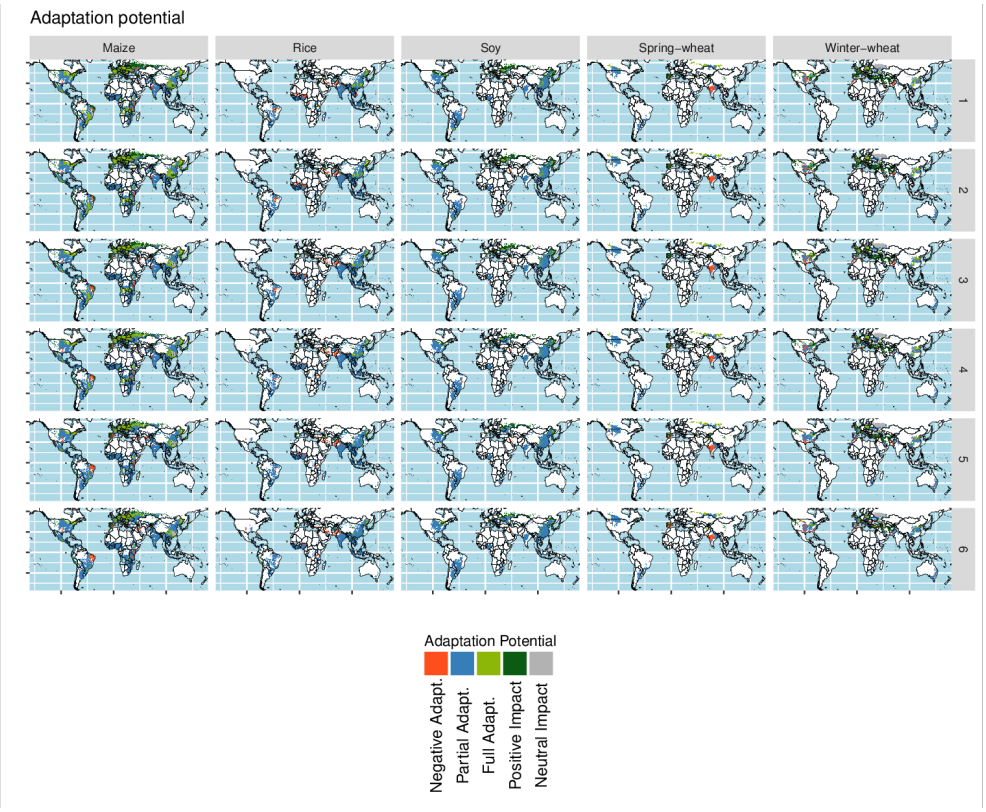

Figure S13: As Figure 4a, but for each temperature offset.

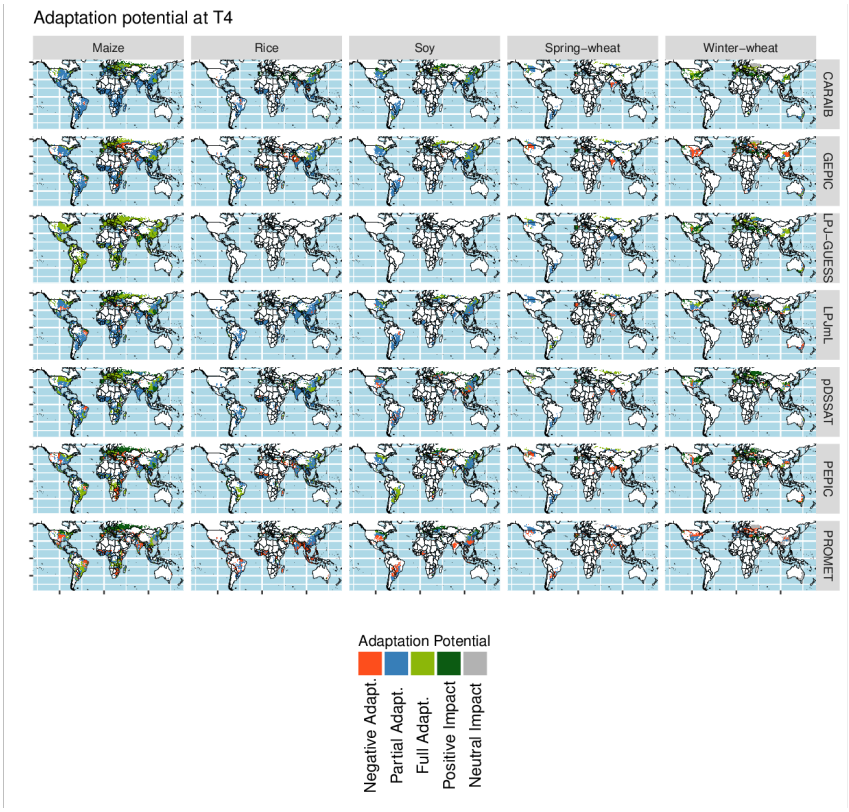

Figure S14: As Figure 4a, but for each GGCM.